MATERIALS FORUM VOLUME 35 – 2011
Edited by P. Howard, P. Huggett and R. Wuhrer

HEAT TREATMENT OF THERMALLY SPRAYED Ni-BASED WEAR AND CORROSION COATINGS

M. Giacomantonio[a,b], S. Gulizia[a], M. Jahedi[a], Y. Wong[b], R. Moore[c], M. Valimberti[c]

[a]CSIRO Materials Science & Engineering, Private Bag 33, Clayton, Victoria 3169
[b]Swinburne University of Technology
[c]United Surface Technologies Pty Ltd

ABSTRACT

Currently there are various types of thermal spray coatings available for wear and corrosion protection and their performance is greatly dependant on the level of porosity inherent in these coatings. This study focuses on Nickel-based coatings produced by Thermal spray technology followed by Flame or Laser heat treatment to produce a dense, well adhered, and relatively porous free microstructure that enhances corrosion and wear resistance. The results show that heat treatment produces a strong metallurgical bond with the substrate which in turn increased the coating adhesion and reduces porosity. A unique coating adhesion test was developed to measure the high coating strengths and the microstructure and mechanical properties compared with coatings produced without heat treatment. It is believed that laser heat treatment of thermal spray coatings can produce cost effective coatings with enhanced corrosion and wear properties for the manufacturing industry.

1. INTRODUCTION

Thermal spray technologies have been widely investigated because of their versatility to deposit metallic, ceramic and composite based coatings that provide thermal, wear and corrosion properties [1]. During thermal spray powder particles are heated to molten or semi-molten state using Flame Spray (FS), Plasma Spray (PS) and High Velocity Oxygen Fuel (HVOF) [2]. Depending on the Thermal spray process used, powder particles can be accelerated to supersonic velocities, forming dense coatings with good wear and corrosion properties [3]. There is however, always a degree of inherent porosity found in thermal spray coatings ranging from <2-20% [4]. Porosity can have a detrimental effect on the performance of anti-corrosion coatings in service because the corrosive media eventually find a path to the substrate [5]. To overcome this shortfall Nickel-based self fluxing alloy powders have been developed for thermal spray applications. These coatings require heating after deposition to fuse the coating which has the effect of increasing the coating adhesion and forming a dense, almost pore free microstructure [6]. Heating is carried out using inductive, or furnace heating but generally a gas torch is applied over the coating until a glassy shine appears indicating the correct fusing temperature has been reached. There is a high degree of operator error during fusing because the temperature envelope required is narrow ranging from the solidus at 950°C to liquidus temperature at 1040°C. Moreover, if the fusing temperature is exceeded, thermal stresses contribute to cracking, excessive distortion of the substrate and coating failure. The high fusing temperatures also limits the choice of substrates that can be used for these coatings. It is not surprising that fusing is generally carried out on relatively small parts and cylinders where heating and distortion can be easily controlled.

In this study laser heat treatment is used to fuse two different Ni-based alloys deposited by FS and HVOF. It is thought that the laser provides a more controlled heating process than gas flame fusing and enables fusing to be carried out on larger parts as well as temperature sensitive substrates, laser fusing also seals coatings and reduce porosity [7, 8]. The results show laser fusing of Ni-based coatings improves porosity and adhesion of coatings produced by FS and HVOF. The mechanical properties and microstructures are also compared to conventional Fusing techniques.

2. MATERIALS AND EXPERIMENTAL

2.1 Coatings & Experimental

Two Ni-based alloy powders available from Sulzer Metco were selected for this study.

1. Metco 36C (Ni 35 (WC 8Ni) 11Cr 2.5B 2.5Fe 2.5Si 0.5C) with particle size of -150 +45 µm
2. Metco 34F (WC 12Co) 33Ni 9Cr 3.5Fe 2Si 2B 0.5C particle size of -53 +15 µm.

Both powder materials were selected because Metco 36C powder has been developed for FS while Metco 34F has a smaller particle size and distribution range and better suited for HVOF applications. These materials also contain WC and Chromium to enhance corrosion and wear properties.

Flame spraying was carried out using a Metco type 5P spray gun and for the HVOF application a Jetkote II system was used. Table 1 shows the process parameters for FS and HVOF coating system used to deposit Ni-based alloy.

Table 1: FS and HVOF spray parameters for each Ni-based alloy used

Deposition Process	Ni-based Powder	Flow Rate/Pressure	Flow Rate/Pressure	Powder Feed Rate/ Pressure
Flame Spray	36C	Oxygen 1.7 m^3/h	Acetylene 0.93m^3/h	9.1 kg/h
Flame Spray	34F	Oxygen 1.6 m^3/h	Acetylene 0.91 m^3/h	4.5 kg/h
HVOF	34F	Oxygen 7050 kPa	LPG 55kPa	#500 kPa

Powder feed rate regulated by changing pressure

In order to determine the effects of different grit size on coating adhesion, a preliminary trial was conducted using brown alumina grit with mesh sizes #16, #24 & # 46. Stainless steel substrates were grit blasted prior to FS or HVOF coating with 36C powder then fused using a gas heating torch. The surface roughness obtained for each sample after grit blasting is shown in Table 2.

Table 2: Surface roughness measurements obtained using different Alumina grit size

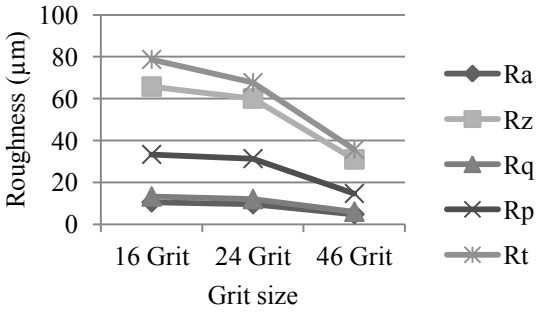

Metallographic analysis was conducted on cross-sectioned samples which were epoxy mounted before grinding and final polishing with 1µm diamond. SEM analysis was conducted using a Leica 440 with Oxford ISIS EDS and Oxford X-Max. LOM images were obtained using an Olympus PMG3 optical microscope and porosity measurements with the image analysis program ImageJ®, whereby images of the coating were scanned for porosity as a percentage of the area. Vickers hardness measurements were obtained before and after fusing using a 10 kg load. To measure the surface roughness a Mahr Perthometer was used over a trace length of 5.4 mm.

2.2. Bond Strength

The ASTM 633 standard on determination of adhesive strength of thermal spray coatings could not be utilised for fused coatings because the glue strength was exceeded. Researchers have previously reported that fused thermal spray coatings [9] achieve high strengths due to the metallurgical bonds achieved during fusing however, no international standard exists to measure the bond strength of fused coatings and there was a need to develop a new test methodology for measuring the adhesion of thermal spray fused coatings.

A new test was developed utilising an Instron® compression testing machine with a specially made attachment that could shear coatings off cylindrical substrates. For this test the circumference of the rods were coated and subsequently fused. After fusing the samples were machined to 5 mm thick with a 2 mm step in the coated area for shearing. A push-rod with dimensions 120x 120 x 25mm^3 was designed to apply a constant load to the coating surface until failure occurred, Fig. 1.

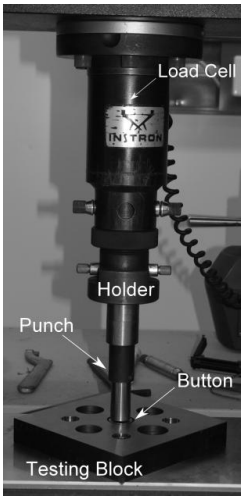

Fig. 1: New adhesion test setup with push-rod and sample in position ready for testing

2.3 Fusing of Thermal Spray Coatings

The conventional method to fuse thermal spray coatings is by gas torch heating. The heat is applied until a shine appears on the surface indicating the optimum fusing temperature range has been reached. The surface temperature can reach in excess of 1000°C during fusing and once the shine appears the gas heating is slowly moved to another area of the coating. Although furnace and inductive fusing has also been reported it is not commonly carried out by the Thermal spray industry. Fig. 2 illustrates the commonly used fusing technique carried out on a cylinder showing three separate gas heating torches applying heat simultaneously to a small area of the coating while the cylinder is being rotated.

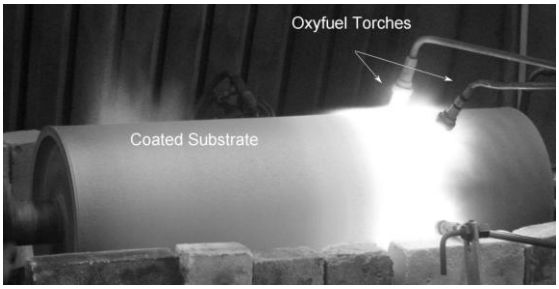

Fig. 2: Flame fusing a cylindrical roller which has been deposited with Ni-based alloy

Laser fusing on the other hand is new and experiments were conducted using a Trumpf POM DMD 505 machine with a CO_2 laser capable of a maximum laser power level of 5 kW. Stand-off distance for the laser beam was 20 mm and a spot size of 3mm was used with 50% overlapping passes. To determine the optimum laser fuse condition, samples were exposed to power levels ranging from 0.25-3 kW in increments shown in Table 1. A laser traverse speed of 500 mm/min was used for all FS and HVOF coatings deposited on flat stainless steel substrates 250 x 75 x 10 mm^3.

Table 3: Laser power settings used for each coating to determine optimum laser fusing conditions.

Laser Power (kW)	0.25	0.5	1	1.5	2	2.5	3

3. RESULTS AND DISCUSSIONS

3.1 Bond Strength

Interestingly, there was only a 10% increase in bond strengths between different grit sizes, 470 MPa for #16 mesh grit to 500 MPa for #46 mesh, Fig. 3. This trend is opposite to what is generally expected for thermal spray coatings because the bonding mechanisms rely on mechanical anchoring and therefore a high surface roughness produced by grit blasting generally produces higher bond strengths. It appears fusing alters the substrate/coating interface such that a metallurgical bond occurs rather than mechanical resulting in approximately 10 times increase in bond strength from thermal spray coatings without fusing.

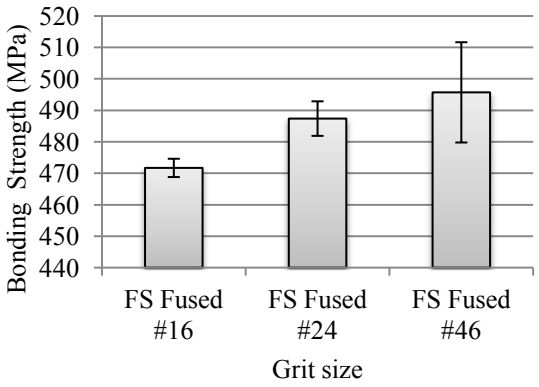

Fig. 3: Graph showing effects of bond strength with grit blast media for 36C coatings produced by FS and gas torch fused.

There was only a moderate difference in bond strength between the coatings produced by FS and HVOF in the as-sprayed conditions. However, the bond strength increased significantly when the coatings were fused, approximately 40 MPa to over 400 MPa respectively, see Fig. 4. All coatings failed in purely shear component as was designed using the new test methodology. Another observation was the coating produced in the as-sprayed condition had a rough appearance at the substrate/coating interface whereas the fused coatings had sheared cleanly at the substrate/coating interface indicating a degree of metallurgical bonding and supports the previous observations, Fig. 5.

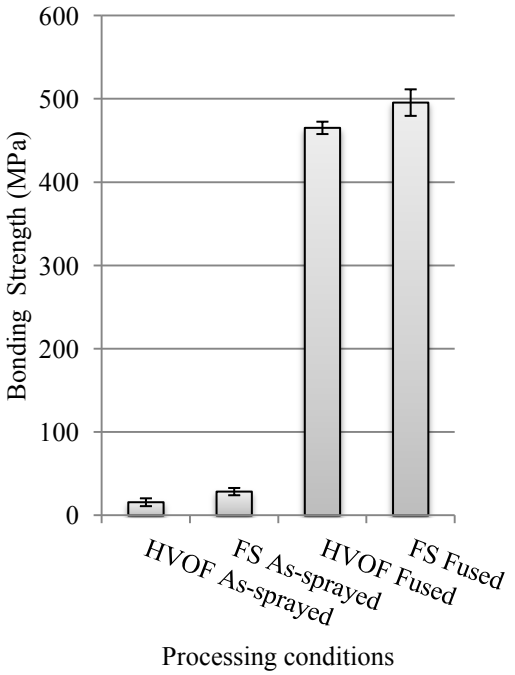

Fig. 4: Comparison of the bond strengths achieved for HVOF and FS in the as-sprayed and fused conditions

Fig. 5: Coated test sample after testing (right) showing coating ring sheared from circumference (left)

3.2 Hardness and Roughness Measurements

The hardness measurements for all Ni-based coatings produced by FS and HVOF and Fused range from 700-900 HV. This is significantly higher than the hardness of FS and HVOF coatings without fusing, measuring <600 HV. Higher hardness levels were obtained in the matrix area where WC was found, ranging from 1000-1100 HV. Such high hardness is expected to be favourable for wear resistance applications.

Roughness measurements of Nickel based coatings produced by FS and HVOF in the as-sprayed and fused conditions are shown in Fig. 6. The surface roughness for the laser fused coatings was lower than the coatings produced in the as-sprayed conditions 10-30 Rz and 50-80 Rz respectively. A smoother coating after fusing can result in significant savings and benefits needed to machine/grind fused coatings to size.

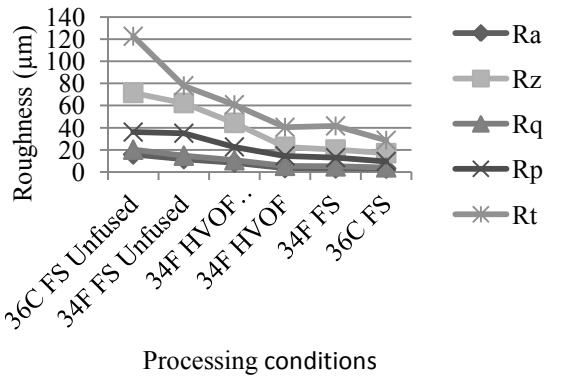

Fig. 6: Surface roughness measurements of 34F and 36C coatings in as-sprayed and Fused conditions

3.3 Microstructural Examination

SEM and optical analysis of the coatings produced by FS and HVOF in the as-sprayed and fused conditions are shown in Fig. 8. A typical lamellar coating structure is observed for all thermal spray coatings showing oxides, splat formation, cracks and porosity distribution within the microstructure. However when coatings were fused the microstructure completely transformed to form a dense relatively pore free coating. The porosity level was also affected for as-sprayed FS and HVOF coatings; the porosity was 6% and 2% respectively compared to fusing where the porosity level reduced to 2% for FS but unexpectedly increased to 8% for HVOF, Fig. 7. It appears operator fusing practice contributed to the porosity increase for the fused HVOF coating highlighting the variability that can be obtained when fusing manually with gas heating. There is also a notable difference in the microstructure of the coatings which were fused by gas heating compared to laser fusing. The laser fusing sample contained less porosity than the samples Fused by gas heating method, see Fig. 8.

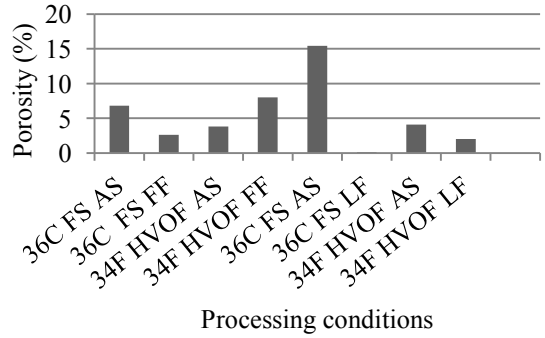

Fig. 7: Porosity as a percentage of the coating (Where AS –As-sprayed, FF- Flame fused and LF-laser fused.)

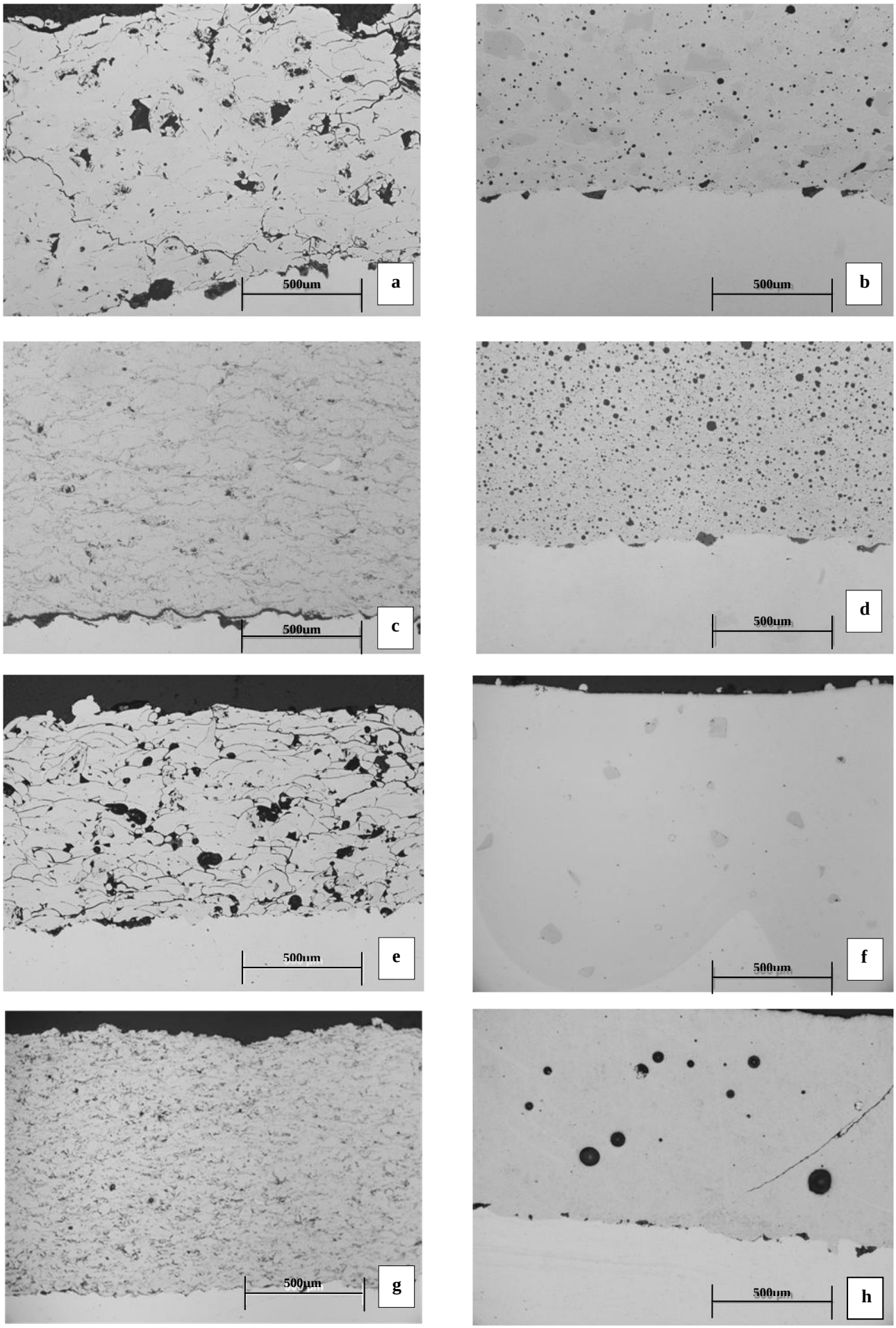

Fig. 8: Optical microscope images of **a)** 36C FS as-sprayed **b)** 36C FS flame fused **c)** 34F HVOF as-sprayed **d)** 34F HVOF flame fused **e)** 36C FS as-sprayed **f)** 36C FS laser fused **g)** 34F HVOF as-sprayed **h)** 34F HVOF laser fused

3.4 Laser Fusing

The effects of laser fusing were apparent soon after heating with some power settings showing excessive heating and melting while others contained significant amount of stress cracking. Fig. 9 is a photograph of the laser fused coatings produced by different laser conditions showing effects on the coating. Furthermore, it showed when <1 kW of laser power was used there was insufficient fusing of the coating and the coating was largely unchanged from the as sprayed condition. When the power was increased to 1-1.5 kW cracks appeared and the coatings mostly spalled and disintegrated when attempting to prepare the sample for metallographic analysis. Coatings within this power range also showed a large number of gas pores which is believed to be a result of the inability of gas to escape during Fusing, Fig. 10. Complete fusion appeared when using 2.5-3 kW laser power. Coatings processed at this level demonstrated a completely fused and pore free (<0.1%) microstructure with even distribution of tungsten carbide in the matrix. These laser fused coatings contain ideal microstructures for enhancing bond strength and corrosion protection.

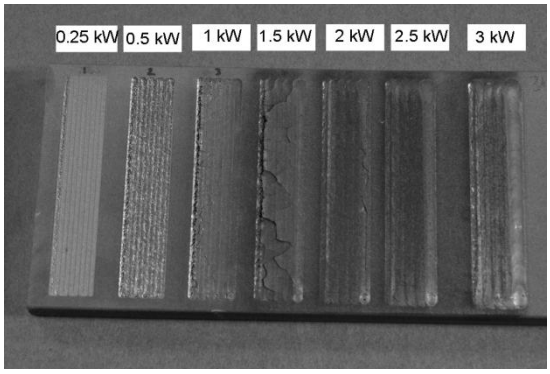

Fig. 9: Coatings produced by Laser Fusing showing visible cracks on coating with various Laser conditions

EDS analysis, Fig. 11, reveal an even distribution of mostly Iron and Nickel in the coating matrix with a presence of Chromium throughout the coating and substrate. Tungsten is also detected in areas within the coating matrix.

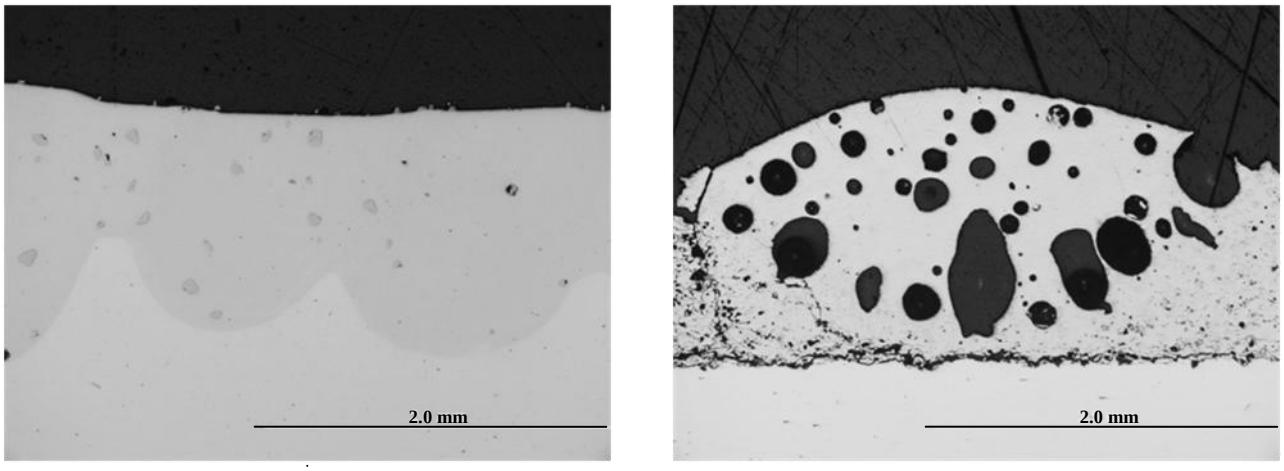

Fig. 10: Laser fused coatings showing a dense mostly pore free coating at 2.5 kW, and a very porous coating at 1 kW.

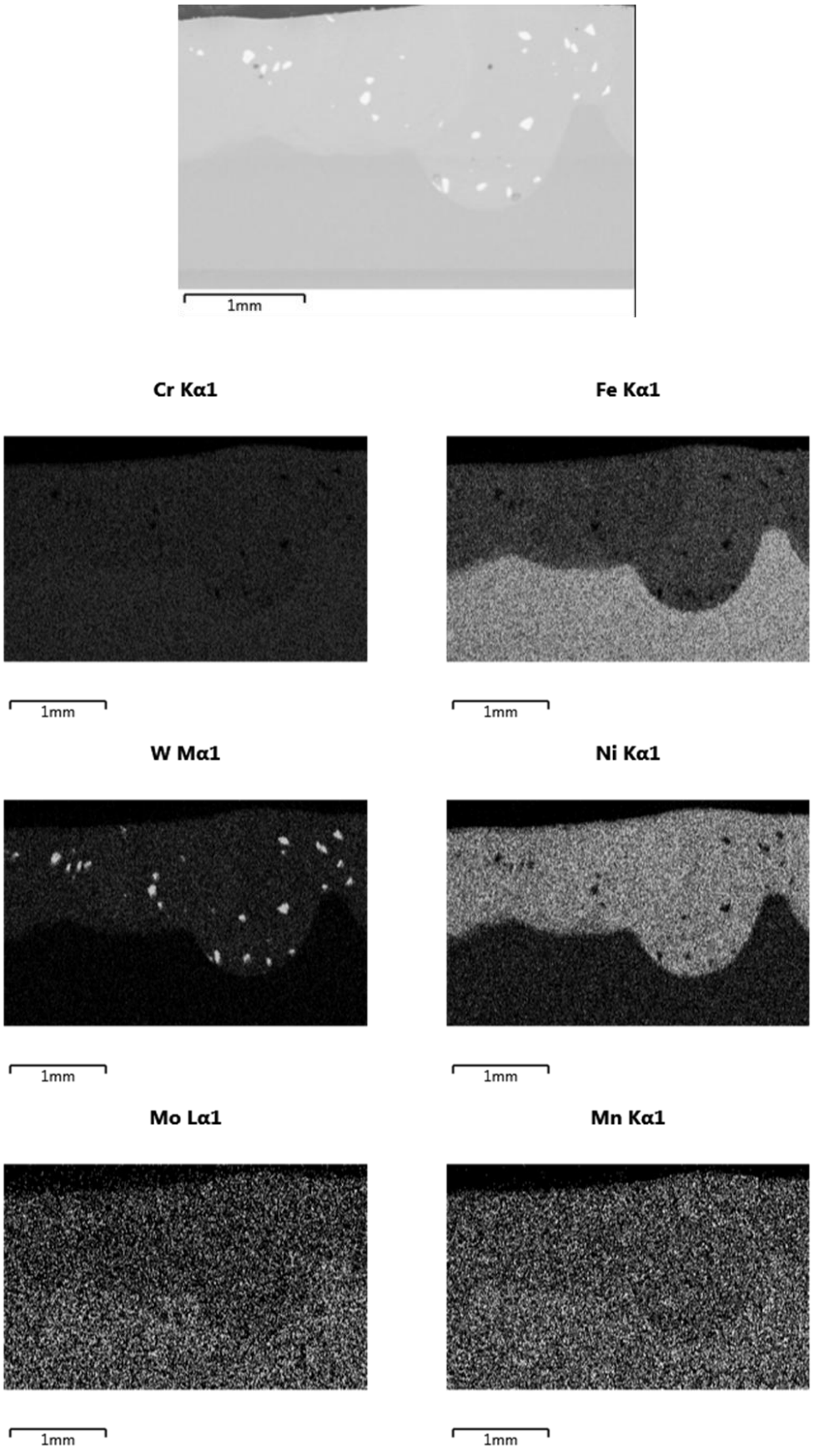

Fig. 11: SEM image of laser fused coating with EDS maps of the distribution of elements present throughout the coating and substrate

4. CONCLUSION

The following conclusions were obtained from this study:

1. Fused coatings demonstrated a 10 time increase in coating bond strengths compared to thermal spray coatings in the as-sprayed condition.
2. Laser fusing transforms the as-sprayed coatings to produce dense porous free microstructures favourable for wear and corrosion resistance applications.
3. The hardness of as-sprayed thermal spray coatings increased from 600HV to 800 HV after laser fusing
4. The surface roughness achieved by laser fusing was lower than for conventional fusing techniques thereby offering potential for large reductions in machining/grinding time.
5. A new coating adhesion test was developed to test fused coatings.

The study identified that by careful selection of laser conditions, fusing thermal spray nickel based coatings can be applied to large parts without spalling, minimised distortion and human error commonly associated with gas heating methods.

ACKNOWLEDGEMENTS

This work was funded by the Victorian Science Agenda (VSA) Direct Manufacturing Centre and supported by United Surface Technologies Pty Ltd. The authors would like to thank Girish Thipperudrappa of Swinburne University of Technology for his assistance with the laser experiments and also Tony Bau, Peter Hawkey and Mark Emmins from United Surface Technologies Pty Ltd who participated in this study.

REFERENCES

[1] S. V. Klinkov, V. F. Kosarev, A. A. Sova, and I. Smurov, "Deposition of multicomponent coatings by Cold Spray," *Surface and Coatings Technology,* vol. 202, pp. 5858-5862, 2008.

[2] F. W. Bach, K. Möhwald, B. Drößler, and L. Engl, "Technology and potential of wear resistant thermal spray coatings," *Materialwissenschaft Und Werkstofftechnik,* vol. 36, pp. 353-359, Aug 2005.

[3] L. Fedrizzi, S. Rossi, R. Cristel, and P. L. Bonora, "Corrosion and wear behaviour of HVOF cermet coatings used to replace hard chromium," *Electrochimica Acta,* vol. 49, pp. 2803-2814, 2004.

[4] X. C. Zhang, B. S. Xu, Y. X. Wu, F. Z. Xuan, and S. T. Tu, "Porosity, mechanical properties, residual stresses of supersonic plasma-sprayed Ni-based alloy coatings prepared at different powder feed rates," *Applied Surface Science,* vol. 254, pp. 3879-3889, 2008.

[5] J. Tuominen, P. Vuoristo, T. Mäntylä, S. Ahmaniemi, J. Vihinen, and P. Andersson, "Corrosion behavior of HVOF-sprayed and Nd-YAG laser-remelted high-chromium, nickel-chromium coatings," *Journal of Thermal Spray Technology,* vol. 11, pp. 233-243, 2002.

[6] Y. Li, K. Nishio, M. Katoh, T. Yamaguchi, and S. Olamine, "Effect of laser fusing on hot corrosion resistance of nickel based self fluxing alloy coating," *Materials Science Forum,* vol. 522-23, p. 8, 2006.

[7] X. H. Tan and J. S. Sun, "Laser remelting modification of HVOF sprayed WC-based cermet coatings," Las Vegas, NV, 2009, pp. 1157-1162.

[8] L. Pawlowski, "Thick laser coatings: A review," *Journal of Thermal Spray Technology,* vol. 8, pp. 279-295, 1999.

[9] F. Otsubo, H. Era, and K. Kishitake, "Interface reaction between nickel-base self-fluxing alloy coating and steel substrate," *Journal of Thermal Spray Technology,* vol. 9, pp. 259-263, 2000.